RESEARCH ARTICLE | DECEMBER 18 2024

Studying evaporating black hole using quantum computation algorithms on IBM quantum processor

Ritu Dhaulakhandi ; Raikhik Das ; Bikash K. Behera ; Felix J. Seo

AIP Advances 14, 125121 (2024)
https://doi.org/10.1063/5.0231558

Studying evaporating black hole using quantum computation algorithms on IBM quantum processor

Cite as: AIP Advances 14, 125121 (2024); doi: 10.1063/5.0231558
Submitted: 27 August 2024 • Accepted: 25 November 2024 •
Published Online: 18 December 2024

Ritu Dhaulakhandi,[1,a] Raikhik Das,[1,b] Bikash K. Behera,[2,c] and Felix J. Seo[3,d]

AFFILIATIONS

[1] Department of Physics, Indian Institute of Science Education and Research, Pune 411008, Maharastra, India
[2] Bikash's Quantum (OPC) Private Limited, Mohanpur, Nadia, Balindi, West Bengal 741246, India
[3] Department of Physics, Hampton University, Hampton, Virginia 23668, USA

[a] ritudhaulakhandi3626@gmail.com
[b] raikhikd@gmail.com
[c] bikas.riki@gmail.com
[d] **Author to whom correspondence should be addressed:** jaetae.seo@hamptonu.edu

ABSTRACT

Analyzing complex quantum systems using quantum computational algorithms is one of the most promising applications of quantum computers. This study focuses on evaluating the performance of a custom variational ansatz in the Variational Quantum Eigensolver (VQE) algorithm compared to predefined ansatzes. To achieve this, we employ the evaporating black hole model as a test bed for our analysis. Using the VQE approach, which integrates quantum and classical computing techniques, we aim to minimize the energy expectation value of the Hamiltonian. By training the circuit parameters of a trial wave function as a parameterized quantum circuit, we determine the upper bound for the ground state energy and assess the optimal variational form. We define a custom ansatz for the VQE protocol and compare its performance with other predefined ansatzes. Additionally, we test the performance of three different classical optimizers to further understand their impact on the VQE algorithm's efficiency and accuracy.

I. INTRODUCTION

Deutsch (1985), Feynman (1982), and Benioff and Manin (1980) were the first to shed light on the field of quantum computing. A quantum mechanical model of Turing machines was provided by Benioff.[1] Concurrently, Manin[2] authored the brilliant work "Computable and Uncomputable," which attracted the interest of numerous quantum physicists. Subsequently, Feynman[3] suggested using quantum computers to simulate models that, for a variety of reasons, could not be simulated by classical computers. The concept of quantum computation was revolutionized by additional contributions made in the field of quantum computing by Deutsch.[4] It was not until a decade later that quantum computing became widely accepted after a special algorithm came up. After Shor's algorithm was developed in 1994, interest in quantum computing and its potential was finally sparked.[5] Investments in the study and development of quantum computing increased as a result.

Practical quantum computers that can execute algorithms like Shor's were made possible by the development of quantum hardware by different companies, such as quantum processors and quantum annealers. The only current drawback is that many quantum protocols implemented on real devices do not provide the desired results (as they suffer from error accumulation) due to the lack of fault-tolerant qubits and effective error-correcting codes. Nevertheless, it has been demonstrated that the noisy systems in use today are effective for solving optimization problems.

A quantum computer is a computing device that utilizes features of quantum mechanics to perform calculations,[6] thereby providing access to computational capacity that would have been

unattainable for a classical computer. Numerous algorithms are employed by quantum computers to solve problems and model quantum systems.[7] Numerous applications in different areas of physics have been triggered by these quantum algorithms.[8–10] Feynman, as previously stated, was the one who first suggested using a quantum computer to solve problems related to quantum mechanics. His primary area of interest was the application of quantum computers to model simulations of quantum systems, as classical computers were unable to handle the intricacies of such models.[11]

Since the evolution of a Hamiltonian requires exponential growth in resources, simulating any general Hamiltonian of a quantum system in a classical computer is challenging. The details of a quantum system as it evolves with respect to certain parameters can be studied thanks to quantum simulation.[12] Quantum cosmology[13–20] and condensed matter physics[21] are just a few of the many physics-related fields in which it finds extensive application. Proceeding with the applications of quantum simulation, Peruzzo *et al.*[22] developed the variational quantum eigensolver (VQE) algorithm, which can be used to estimate the ground state energy of a quantum system, an important quantity in quantum chemistry and condensed matter physics. In this work, we investigate the performance of the variational quantum eigensolver (VQE) algorithm for the Evaporating Black Hole (EBH) model on the IBMQ experience platform.[23] With the IBMQ experience, we can use quantum devices to carry out computation tasks from distant locations all over the world.

Research into the quantum theory of gravity and the intersection of gravitation, quantum theory, and thermodynamics has been greatly influenced by Hawking's discovery[24] that a black hole emits particles akin to those produced by a black body with a temperature linked to its surface gravity. Much effort has gone into expanding Hawking's research to produce dynamically evaporating black hole spacetime (hereafter referred to as "EBH spacetime") that is self-consistent and accurate in quantum mechanics, but little progress has been made in this direction. To date, only a semi-classical working field theory for Hawking radiation derivation has been developed. Usually, the Vaidya metric is used to construct classical spacetimes with EBHs. These model EBH spacetimes have event horizons with finite lifetimes that are asymptotically flat and spherically symmetric. Then, these model EBH spacetimes are used as preset backgrounds for particle-creation calculations, hoping to learn something about the dynamics of actual, semi-classical EBH spacetimes, avoiding the difficulties posed by the back-reaction problem.

An EBH toy model is used in this article for the implementation of the VQE algorithm[22] from the Qiskit Aqua library[25] to determine the upper bound of the Hamiltonian's ground state eigenvalue. The EBH toy model was selected mainly due to the fact that it is well studied and, hence, we have enough literature to cross-check the performance of the VQE protocol. Additionally, the library offers an exact eigensolver that facilitates the comparison of the true value of ground state energy eigenvalue and the outcomes of the VQE algorithm. The Hamiltonian needed for the algorithm is obtained using the Schwarzschild metric and the principle of least action. The VQE algorithm is then used to find the upper bound for the Hamiltonian's energy eigenvalue.

The remaining portions of the paper are organized as follows: The entire methodology—from obtaining the EBH model to the steps required for additional quantum algorithm implementation—is provided in Sec. II. Section III contains the results for the different protocol configurations. Sections IV and V offer a comprehensive analysis of the findings, as well as a prospective outlook and concluding remarks.

II. METHODOLOGY

A. Evaporating black hole

Understanding the interplay between quantum theory and gravity is crucial to comprehend the physics of black holes. The Hawking radiation theory, which describes how black holes emit particles, is a key idea in this area. The synthesis of quantum and classical physics serves as the basis for this theory. However, because of their powerful gravitational force, black holes display spatial curvature. When analyzing quantum fields, which are made up of particles and their interactions, we typically assume that they reside in flat background geometry. However, the curvature of spacetime has some interesting effects when quantum fields are studied near a black hole.

In the presence of a black hole, particles can be generated from nothing. This is the result of quantum field fluctuations brought on by the strong gravitational attraction of the black hole. The presence of the black hole may result in a nonzero expectation value for the stress–energy tensor, which measures the quantum fields' momentum and energy. Using the Christensen and Fulling framework, researchers have computed the expected value of the stress–energy tensor outside the event horizon of a black hole. This calculation helps us understand how black holes behave and radiate because it accounts for the effects of quantum fields and gravity. More details regarding the body of work on evaporating black holes are available in the cited references.

Black holes can classically absorb particles but cannot emit particles. However, black holes behave like a hot bath because of quantum phenomena. It can be demonstrated that black holes cause particles to be created and emitted. This causes the mass of the black hole to gradually decrease over time. The term "evaporation of black hole" describes this phenomenon.

A black hole that is evaporating loses mass over time as a result of Hawking radiation emission. To simulate EBH, we can use a semi-classical approach. We only attempt to simulate the EBH's behavior in the early time domain because, in the late time domain, when the EBH has almost entirely evaporated, we encounter quantum gravity-related issues that physicists have yet to resolve. However, at the beginning of the evaporation, we can use approximate semi-classical methods. Hawking provided a semi-classical analysis of Becken–Stein's theory, according to which the surface area of an event horizon black hole is correlated with its entropy and surface gravity. Hawking's analysis was based on quantum field theoretic computations. It is shown that massless particles, mainly photons, are generated in the curved spacetime close to the black hole and escape to I^+ as a result of the Unruh effect. This is observable as alleged Hawking radiation.

Later, Hawking presented a different interpretation of Hawking radiation. He discusses the formation of particle and anti-particle pairs as a result of quantum disturbances near a black hole. The emitted null geodesics are followed by the positive frequency particles.

Quantum tunneling causes the negative frequency particles to enter the black hole, which reduces the black hole's mass.

If one tries to construct a simple representation of the EBH spacetime, one may assume spatial symmetry, which would cause the metric components to rely on time in a manner that would describe the EBH's mass loss profile. Aste and Trautmann changed the Schwarzschild metric's mass term to depend on time in a simplified model they created in 2005.[26] We will be working in similar environments in this work. Schwarzschild metric describes the spacetime resulting from uncharged, non-rotating black holes. The Schwarzschild metric has the following form in polar coordinates:

$$ds^2 = -c^2\left(1 - \frac{r_s}{r}\right)dt^2 + \left(1 - \frac{r_s}{r}\right)^{-1} dr^2 + r^2\, d\theta^2 + r^2 \sin^2\theta\, d\phi^2, \quad (1)$$

where the Schwarzschild radius is denoted by $r_s = \frac{2GM}{c^2}$. M represents the black hole's mass. However, the mass of a Schwarzschild black hole is constant, meaning that the spacetime solution of Einstein's equations yields a stationary metric. That is not the case for EBH. The black hole mass term for EBH will be non-constant. It goes without saying that the black hole's mass will fluctuate over time as the EBH emits energy. We will work with a very simple model of EBH. In our model, the metric for spherically symmetric evaporating black holes in polar coordinates is

$$ds^2 = -c^2\left(1 - \frac{r_s(t)}{r}\right)dt^2 + \left(1 - \frac{r_s(t)}{r}\right)^{-1} dr^2 + r^2\, d\theta^2 + r^2 \sin^2\theta\, d\phi^2. \quad (2)$$

After deciding on a model, the next step is to determine the system's Hamiltonian. The system will consist of Hawking radiation and spacetime itself if we take the entire system outside of EBH into consideration. Hence,

$$S = S_{spacetime} + S_{matter}, \quad (3)$$

where S = action of the whole system outside EBH, $S_{spacetime}$ = action due to the spacetime, and S_{matter} = action due to the Hawking radiation.

One way to conceptualize the Hawking radiation action is as a field action. Massless scalar fields have been widely used to characterize Hawking radiation in the extensive body of research on the phenomenon. Therefore, one can consider the action for a massless field for S_{matter}. On the other hand, the expression for $S_{spacetime}$ is as follows:

$$S_{spacetime} = \int d^4x\sqrt{-g(x)}R(x), \quad (4)$$

where $\sqrt{-g(x)} = \sqrt{-\det(g(x))}$, and the Ricci scalar for the spacetime under consideration is $R(x)$. In this article, we will only work with a patch of the spacetime. Our system will span from $r = 1.5r_s(t)$ to $r = 2r_s(t)$. The patch under consideration appears arbitrary at first glance, but it is significant because the "quantum atmosphere," which is responsible for the majority of particle–antiparticle pairs, has been estimated to span radially from 1.5 to 2 Schwarzschild radii,[27] based on a 1 + 1 dimensional calculation. In an effort to streamline our analysis, we will only consider an isolated system—that is the background spacetime—rather than the entire system, which would be background spacetime + Hawking radiation. It is also reasonable to wonder if, in doing so, we are likewise ignoring the consequences of spacetime and Hawking radiation interactions. However, we will only work with the spacetime patch spanning from $r = 1.5r_s(t)$ to $r = 2r_s(t)$ in order to simplify our system as much as possible. From now on we will suppress the subscript "*spacetime*" in $S_{spacetime}$ and write

$$S = \int d^4x\,\mathcal{L}(x), \quad (5)$$

where the Lagrangian density is $\mathcal{L} = \sqrt{-g(x)}R(x)$. Using the metric in Eq. (2), we get

$$\sqrt{-g(x)} = r^2 \sin\theta, \quad R(x) = \frac{r\left(2\dot{r}_s^2 + (r - r_s\ddot{r}_s)\right\}}{c^2(r - r_s)^3}, \quad (6)$$

where $\dot{r}_s = \frac{dr_s(t)}{dt}$. Using Eq. (6), we calculate the Lagrangian for our system

$$\begin{aligned} L &= \int d^3x\,\mathcal{L} \\ &= \int_0^{2\pi} d\phi \int_0^{\pi} d\theta \\ &\quad \times \int_{1.5r_s(t)}^{2r_s(t)} dr\, r^2 \sin\theta\left(\frac{r\left(2\dot{r}_s{}^2(t) + (r - r_s(t))\ddot{r}_s(t)\right\}}{c^2(r - r_s(t))^3}\right) \\ &\simeq \frac{2\pi}{c} r_s(t)\left(28.3178\dot{r}_s{}^2(t) + 9.908\,88\, r_s(t)\,\ddot{r}_s(t)\right). \end{aligned} \quad (7)$$

Now, we will do a new parameterization: $X(t) = [r_s(t)]$.[2] He the Lagrangian takes the following form:

$$L \simeq \frac{1}{c}\left(65.2427\,\dot{X}^2 + 41.5062\,X\ddot{X}\right). \quad (8)$$

The Lagrangian in Eq. (8) leads to the following Hamiltonian:

$$H \simeq \frac{65.2427}{c}\dot{X}^2. \quad (9)$$

Now that the Hamiltonian [Eq. (9)] of the EBH toy model is ready, we have to map it into a discrete space system Hamiltonian in order to implement the VQE protocol.

In our toy model, we considered the black hole to be non-rotating and the metric to be spatially symmetric. So, we have taken the Schwarzschild metric and made the radius of the black hole horizon dependent on time. However, this metric ansatz has shortcomings. This model is not entirely accurate since there is no relationship between time inside and outside of a black hole. This is because the model loses all physical meaning at the horizon when the time coordinate expands into infinity.

During the late-time behavior of the black hole, our semi-classical analysis breaks down as the quantum effects become powerful. Hence, one has to consider quantum gravity for late-time analysis of EBH. In this work, we strictly avoid the late-time radiation scenario due to limitations in quantum resources (discussed in more detail in Sec. III).

The Vaidya metric is a time-dependent, spherically sym-metric mass distribution that can absorb or emit radiation; as such, physicists have frequently used it to describe the space-time structure

outside of EBH.[28–32] However, our goal in this work is to consider the effect of spacetime near the horizon of the evaporating black hole. We have not considered the effect due to the Hawking radiation. For this exact reason, we have considered this toy model instead of the Vaidya metric (a more realistic metric for EBH), as the Ricci scalar of the Vaidya metric is zero. In the case of the Vaidya metric, the Hamiltonian is purely a result of Hawking radiation. Hence, our method of analysis is rendered unfruitful in the case of the Vaidya metric. However, our future direction, briefly mentioned in Sec. IV, can solve this issue.

B. Discretization of space

The Hamiltonian obtained for the EBH model [Eq. (9)] has a continuous eigenspectrum. To simulate it on a quantum computer, it needs to be mapped to a discrete space system representation.[33] To accomplish this, a discretized two-dimensional space with $x, y \in [-L, L]$ and N eigenvalues for each of x and y is described. This produces a mesh with N^2 spatial elements, where each element is associated with a unique eigenvalue that is determined by the element's x and y values. With the mesh centered at [0, 0], the discrete position operator[34] has the following $N \times N$ matrix, with position eigenvalues located along the diagonal:

$$x^d = \sqrt{\left(\frac{\pi}{2N}\right)} \begin{bmatrix} (-N/2) & 0 & 0 & \cdot & \cdot & 0 \\ 0 & (-N/2)+1 & 0 & \cdot & \cdot & 0 \\ 0 & \cdot & \cdot & \cdot & \cdot & \cdot \\ 0 & \cdot & \cdot & \cdot & \cdot & \cdot \\ \cdot & \cdot & \cdot & \cdot & \cdot & 0 \\ 0 & 0 & 0 & \cdot & 0 & (N/2)-1 \end{bmatrix}. \tag{10}$$

The momentum operator can be obtained by taking the Fourier transform of the x^d (position operator).[35] The following is the momentum operator:

$$p^d = (F^d)^{-1} x^d F^d, \tag{11}$$

where the elements of the matrix F^d, which represents the quantum Fourier transform, are as follows:

$$\left[F^d\right]_{j,k} = \frac{\exp\left(i2\pi jk/N\right)}{N^{1/2}}. \tag{12}$$

With the position operator and momentum operator now in hand, all that is left to do is select a value for N to obtain the Hamiltonian in matrix form. For the systems where $N = 2$, 4, 8, and 16, we will work. As N increases, the discrete space operator indicates that both the number of spatial points in the mesh and the number of qubits needed to run the simulation will increase. For very high values of N, the simulation should, in theory, be more accurate because it should be closer to the real model. However, more qubits in the system mean that the ansatz needs to contain more parameters in order to find the ground state wave function.

For a range of N values, the discrete space system Hamiltonian for the Hamiltonian given in Eq. (9) is obtained and utilized as an input for the VQE algorithm. The VQE protocol's operation and the different components involved in determining the upper bound of the ground state energy eigenvalue must now be described before moving forward with implementation.

C. Variational quantum eigensolver (VQE) algorithm

The state of the quantum system is described by the wave function. Moreover, a normalized wave function can be expressed as a superposition of its eigenstates,

$$|\psi\rangle = \sum c_n |\psi_n\rangle, \tag{13}$$

where $\langle\psi|\,\psi\rangle = \sum |c_n|^2 = 1$ and $H\,|\psi_n\rangle = E_n\,|\psi_n\rangle$.

The Hamiltonian's expectation value can be expressed in the following way:

$$<H> = <\psi|H|\psi> = \sum E_n |c_n|^2. \tag{14}$$

It is established that the ground state energy of a system E_g is either equal to or less than E_n ($E_g \le E_n$). Consequently, we derive the following from quantum mechanics' variational principle:[6]

$$\begin{aligned} \sum E_g |c_n|^2 \le \sum E_n |c_n|^2 &\Rightarrow E_g \sum |c_n|^2 \le \sum E_n |c_n|^2 \\ &\Rightarrow E_g \le \sum E_n |c_n|^2. \end{aligned} \tag{15}$$

Ansatz, which is a parameterized quantum circuit with parameters that are updated after every run, is built initially for the supplied Hamiltonian in the variational quantum eigensolver (VQE)[22] algorithm. Although the user has the ability to change them, the parameters of the ansatz for the first run are typically initialized as random numbers. Sufficient flexibility is required in the ansatz to prevent the desired state from being overlooked. If the ansatz is not chosen appropriately, the process may end at less-than-ideal parameters that do not correspond to minima. The algorithm is said to have hit a "barren plateau" in this case. The ansatz is the trial function $\psi(\vec{\theta})$ used at the beginning of the algorithm. Following the application of the ansatz, the Hamiltonian is appended, and measurements are obtained in order to calculate the energy ($E(\vec{\theta})$) expectation value. Given that the parameterized state has variables that can be changed, one can be sure to find the parameterized state that is closest to the ground state of the Hamiltonian based on the variational method of quantum mechanics. The parameters of the ansatz are optimized via classical techniques. Finding a multivariable function's minima is required for this minimization. Three different classical optimizers provided by Qiskit are used for this purpose. The circuit is run many times while constantly updating the parameters of the ansatz until the global minima is obtained. The parameters corresponding to the global minima found are saved as the optimal parameters for the given ansatz. An upper bound for the energy eigenvalue (E_g) is obtained by implementing the entire protocol. An outline of the VQE algorithm can be found in Fig. 1 and Algorithm 1.

D. Thermal noise model

The main challenge in developing large-scale quantum computers and carrying out lengthy quantum computations is noise. It is either caused by unintended interactions with the environment (such as thermal, electromagnetic, or gravitational decoherence) or by flaws in the quantum hardware (such as gates and measuring devices).

Irreversible interactions between the quantum system and its surroundings are one of the main sources of errors. This kind

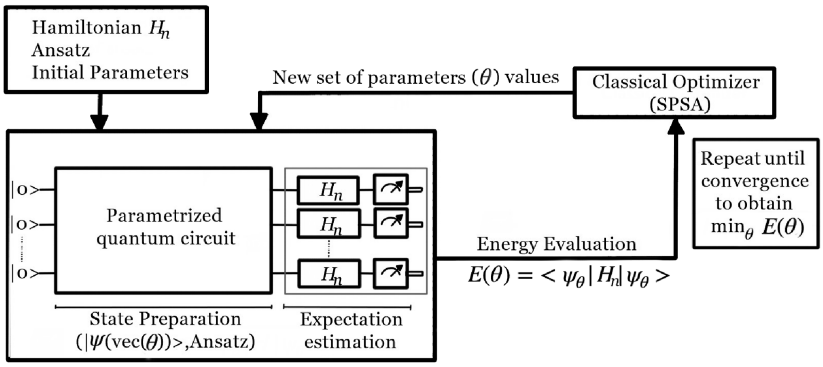

FIG. 1. An illustration of the VQE algorithm's execution is shown here. For a given parameterized trial wave function of a Hamiltonian, the optimal ground state configuration can be found using the VQE algorithm. The trial function used in the algorithm's initialization is called the ansatz (parameterized quantum circuit). Following the addition of the Hamiltonian, measurements are taken in order to determine the Hamiltonian's expectation value. Utilizing three distinct classical optimizers supplied by Qiskit, the ansatz parameters are optimized via classical techniques. The circuit is repeatedly operated upon, with the ansatz parameters updated continuously, until the global minima are achieved. For each ansatz, the optimal parameters are those that correspond to the global minima and are saved.

of noise results in decoherence during computation in a variety of ways. The most prevalent one, which is also the one that is used in our model, is thermal relaxation or excitation. Since such quantum noise is irreversible, it is challenging to replicate it using Pauli or Clifford operations, necessitating a more complicated strategy. Other types of decoherence, such as electromagnetic or gravitational, are not taken into account in this article.

Thermal error contains thermal decoherence (or relaxation), which develops over time as excitation or deexcitation. Thermal relaxation is the irreversible process of qubit spin thermalization to an equilibrium state at ambient temperature. Energy is exchanged between the qubits and their environment during this process, which pushes the qubits in the direction of either the excited state, $|1\rangle$, or the ground state, $|0\rangle$. Conversely, dephasing characterizes the processes by which coherence deteriorates over time. It is a method that explains the transition of a quantum system from quantum to classical behavior.

ALGORITHM 1. VQE algorithm.

Input: Discrete space system Hamiltonian. Ansatz (parameterized quantum circuit). Initial parameters
Output: Upper bound for ground state energy.
The VQE algorithm follows the following steps
Step-1: The ansatz is first applied to the quantum circuit, followed by the Hamiltonian operator
Step-2: Measurements are obtained to find the energy expectation value of the Hamiltonian operator for the given ansatz
Step 3: The optimizers use different techniques to update the parameters and get closer to the ground state
Step 4: Steps 1, 2, and 3 get repeated with the updated parameter values until the global minima is obtained, i.e., the parameterized state (ansatz) is closest to the ground state of the given Hamiltonian

This error group is already implemented as a quantum channel by a function in Qiskit. The following factors are taken into account by the model:

- The mean time of execution, denoted as T_g, for every kind of quantum gate implemented, g.
- The relaxation and dephasing times of a single qubit q, which are commonly represented as $T_1(q)$ and $T_2(q)$, respectively, for $q \in [0, n-1]$, where n is the total number of qubits in the quantum computer.

For each qubit, the behavior of the off-diagonal elements over time is indicated by $T_2(q)$, which indicates a gradual perturbation along the quantization axis (z component of the Bloch vector). $T_1(q)$ represents a progression toward equilibrium as a perturbation orthogonal to the quantization axis (x, y component of the Bloch vector). $T_2(q) \leq 2T_1(q)$ describes the relationship between these two times. When a gate of type g is applied to a qubit q, the probability that it will relax and dephase is given by $p_{T_1(q)} = e - T_g/T_1(q)$ and $p_{T_2(q)} = e - T_g/T_2(q)$, respectively. Then, $p_{reset}(q) = 1 - p_{T_1(q)}$ defines the probability that a qubit would reset to an equilibrium state.

III. RESULTS

The EBH model used in this article only accounts for the early behavior of the EBH, as later dissipation raises quantum gravity-related problems. The EBH model is simple and built assuming spatial symmetry of spacetime. This means that the metric components are dependent upon time in a way that describes the mass loss profile of the EBH.

Various predefined ansatz provided by the Qiskit library were tested out, from which the TwoLocal ansatz performed the best. The parameterized TwoLocal circuit has layers that alternate between rotation and entanglement. All of the qubits have single qubit gates applied to them to create the rotating layers. The user-configurable entanglement approach is carried out by the two-qubit gates in the entanglement layer. In this article, the default full entanglement configuration is used, which entangles every qubit with every

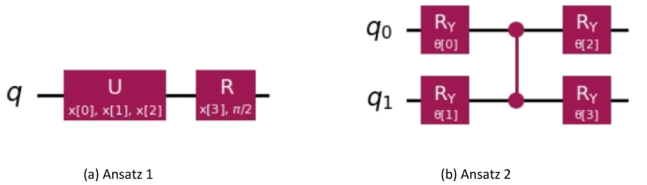

FIG. 2. (a) The U_3 gate is applied in ansatz 1 first, and then a *Ry* gate. This combination is iterated twice for all implementations of the VQE protocol. (b) Ansatz 2 is the predefined TwoLocal ansatz provided by the Qiskit library. The iteration for this ansatz is also set as twice for all implementations of the VQE protocol.

other qubit. A custom ansatz is also used to implement the VQE protocol. The repeating unit of the custom ansatz used is defined as follows:

$$R_y(\theta')U_3(\theta,\phi,\lambda) = \begin{bmatrix} \cos\frac{\theta'}{2} & -\sin\frac{\theta'}{2} \\ \sin\frac{\theta'}{2} & \cos\frac{\theta'}{2} \end{bmatrix} \begin{bmatrix} \cos\frac{\theta}{2} & -e^{i\lambda}\sin\frac{\theta}{2} \\ e^{i\phi}\sin\frac{\theta}{2} & e^{i\phi+i\lambda}\cos\frac{\theta}{2} \end{bmatrix}. \tag{16}$$

Figure 2 shows the custom ansatz repeat unit for a one-qubit system and TwoLocal ansatz repeating unit for two qubit systems. The TwoLocal ansatz for one-qubit system is simply the R_y rotation gate. A custom ansatz using a combination of U_3 and R_y gates in a VQE protocol offers distinct advantages over standard Qiskit ansatz options for simulating the Hamiltonian of an EBH, where spacetime dynamics require precise control and expressibility to capture the underlying physics. By limiting unnecessary entanglement and targeting specific qubit rotations, this ansatz reduces the parameter space to the essential degrees of freedom, optimizing computational resources while retaining fidelity to the EBH dynamics. This precision reduces circuit depth and minimizes noise, which is advantageous given current quantum processor limitations.

The three optimizers used for VQE protocols are COBYLA, L-BFGS-B, and Sequential Least SQuares Programming (SLSQP) optimizer. Michael J. D. Powell developed the numerical optimization technique known as constrained optimization by linear approximation (COBYLA) for constrained problems where the objective function's derivative is unknown. Minimizing the value of a differentiable scalar function f is the primary goal of the Limited-memory Broyden–Fletcher–Goldfarb–Shanno Bound (L-BFGS-B) algorithm. This optimizer employs a quasi-Newton technique to find the minimal value of *f*. Unlike Newton's method, it does not require the Hessian, which is the matrix of f's second derivatives. A function of many variables is minimized by SLSQP under any arrangement of limits, equality, and inequality constraints. When the objective function and the constraints are twice continuously differentiable, SLSQP is the best solution. For the noisy model, the VQE protocol is implemented with the estimator set to replicate the behavior of the thermal noise model.

The first result is for the one-qubit system, or $N = 2$. The discrete space system Hamiltonian is given as

$$H = \begin{bmatrix} 102.482\,993 & 102.482\,993 \\ 102.482\,993 & 102.482\,993 \end{bmatrix}. \tag{17}$$

This Hamiltonian is used in the form of an operator input for the VQE protocol. From Tables I and II, it can be observed that the L-BFGS-B optimizer gave the upper bound value closest to the actual ground state energy, with the custom ansatz result being equal to the actual energy value. In addition, the optimizers, in general, gave better upper bounds for custom ansatz compared to TwoLocal ansatz. However, for the noise model, it can be seen that the TwoLocal ansatz worked better as the custom ansatz reached the barren plateau early and stopped further iterations. The custom ansatz has a higher cost function evaluation than the TwoLocal ansatz, and the optimization time is also double because of the higher number of parameters. The optimal parameter values for the two ansatz are also provided in the Tables for $N = 2$.

TABLE I. VQE result for $N = 2$ and custom ansatz.

VQE performance parameters	COBYLA	L_BFGS_B	SLSQP	COBYLA: Thermal noise model
Eigenvalue	5.6686×10^{-7}	0.0	7.1054×10^{-13}	5.0041
Cost function evals	110	63	80	64
Optimizer time	0.3098	0.1583	0.1914	0.6416
Optimal parameter ($x[0]$)	4.7099	4.2478	6.6217	4.3811
Optimal parameter ($x[1]$)	4.4503	4.0795	3.8286	7.1175
Optimal parameter ($x[2]$)	0.6029	0.6020	0.6020	4.5132
Optimal parameter ($x[3]$)	5.8517	5.4751	3.9786	5.9910
Optimal parameter ($x[4]$)	−2.1869	−3.2780	−2.5158	−3.8096
Optimal parameter ($x[5]$)	1.8207	1.6851	0.7794	5.7907
Optimal parameter ($x[6]$)	−5.4889	−5.4147	−5.2756	−4.6201
Optimal parameter ($x[7]$)	0.5104	0.0578	−2.4910	−6.2370

TABLE II. VQE result for $N = 2$ and TwoLocal ansatz.

VQE performance parameters	COBYLA	L_BFGS_B	SLSQP	COBYLA: Thermal noise model
Eigenvalue	7.6681×10^{-10}	2.4970×10^{-12}	5.2107×10^{-11}	0.0044
Cost function evals	40	28	26	28
Optimizer time	0.1079	0.0748	0.0765	0.4510
Optimal parameter ($\vartheta[0]$)	4.0062	6.5692	4.4748	5.0721
Optimal parameter ($\vartheta[1]$)	5.4760	7.1503	5.0559	6.5665
Optimal parameter ($\vartheta[2]$)	1.5135	3.5593	1.4649	5.6661

TABLE III. VQE result for $N = 4$ and custom ansatz.

VQE performance parameters	COBYLA	L_BFGS_B	SLSQP	COBYLA: Thermal noise model
Eigenvalue	3.5659×10^{-7}	9.9476×10^{-14}	1.3421×10^{-7}	12.2099
Cost function evals	233	221	416	137
Optimizer time	0.9734	0.9499	1.7885	1.7502

The discrete space system Hamiltonian for $N = 4$, i.e., two qubit system, is given as follows:

$$H = \begin{bmatrix} 153.724\,490 & 102.482\,993 & 51.241\,496 & 102.482\,993 \\ 102.482\,993 & 153.724\,490 & 102.482\,993 & 51.241\,496 \\ 51.241\,496 & 102.482\,993 & 153.724\,490 & 102.482\,993 \\ 102.482\,993 & 51.241\,496 & 102.482\,993 & 153.724\,490 \end{bmatrix}. \tag{18}$$

The Hamiltonian in Eq. (18) is taken in as the input Hamiltonian operator for the VQE protocol. From Tables III and IV, the upper bound obtained from the L-BFGS-B optimizer is closer to the actual value for custom ansatz while compromising on the cost function evals and optimization time. However, the overall performance of the COBYLA optimizer is better for the TwoLocal ansatz this time. The upper bound obtained from the SLSQP optimizer is of the same order for the two ansatz; hence, the TwoLocal ansatz has a better overall performance. Since there are more parameters than qubits, the optimal values are not given for higher N, but they can be requested individually, just in case.

The discrete space system Hamiltonian for $N = 8$ and 16 is not explicitly mentioned. However, following the directions provided in the methodology section, they can be calculated easily. From Tables V and VI, it is apparent that the L-BFGS-B and SLSQP optimizers give a closer upper bound value for custom ansatz. However, COBYLA performed better with the TwoLocal ansatz. This is the same for $N = 16$, as seen from Tables VII and VIII, with the only difference being that the SLSQP optimizer gave an almost similar upper bound value. Figures 3 and 4 provide the plots for the upper

TABLE IV. VQE result for $N = 4$ and TwoLocal ansatz.

VQE performance parameters	COBYLA	L_BFGS_B	SLSQP	COBYLA: Thermal noise model
Eigenvalue	1.9068×10^{-9}	1.8341×10^{-11}	4.3341×10^{-7}	0.0110
Cost function evals	128	147	101	58
Optimizer time	0.5778	0.7233	0.4982	0.9071

TABLE V. VQE result for $N = 8$ and custom ansatz.

VQE performance parameters	COBYLA	L_BFGS_B	SLSQP	COBYLA: Thermal noise model
Eigenvalue	1.0950×10^{-6}	3.6734×10^{-13}	8.5378×10^{-9}	76.2434
Cost function evals	435	450	656	271
Optimizer time	4.4575	4.5689	6.8881	5.8686

TABLE VI. VQE result for $N = 8$ and TwoLocal ansatz.

VQE performance parameters	COBYLA	L_BFGS_B	SLSQP	COBYLA: Thermal noise model
Eigenvalue	7.4639×10^{-8}	2.8348e-10	1.8818×10^{-7}	0.0590
Cost function evals	975	200	241	111
Optimizer time	10.6570	2.2315	2.6760	2.8914

TABLE VII. VQE result for $N = 16$ and custom ansatz.

VQE performance parameters	COBYLA	L_BFGS_B	SLSQP	COBYLA: Thermal noise model
Eigenvalue	25.6208	6.0424×10^{-14}	1.0030×10^{-7}	50.7473
Cost function evals	742	1716	1006	341
Optimizer time	25.0128	58.5081	34.3326	18.0251

TABLE VIII. VQE result for $N = 16$ and TwoLocal ansatz.

VQE performance parameters	COBYLA	L_BFGS_B	SLSQP	COBYLA: Thermal noise model
Eigenvalue	8.6194×10^{-8}	6.0897×10^{-11}	1.1256×10^{-7}	0.1310
Cost function evals	847	624	629	144
Optimizer time	29.2660	21.5168	21.6713	7.8537

bound value calculated at each step by the various optimizers, along with the number of iterations to achieve convergence. It can be seen that for the custom ansatz, the COBYLA optimizer reaches a barren plateau and stops iterating further.

A. Mitigation strategies for barren plateaus

It can be seen from Figs. 3 and 4 that barren plateaus are a constant issue faced during optimization. The optimizers converge differently for custom ansatz (with early plateaus for COBYLA, as seen in Fig. 3). Initializing parameters strategically, such as setting parts of the circuit to the identity or using Bayesian optimization or beta distributions, can prevent early stage gradient vanishing and improve gradient flow.[36,37]

Barren plateaus arising due to optimization steps can be prevented by using adaptive optimizers or momentum-based methods, enabling better traversal of flat regions in the optimization landscape with dynamic learning rates that adjust to gradient patterns. Perturbations added during gradient descent further encourage the optimizer to escape flat areas, facilitating gradient retention and optimization progress.

The custom ansatz used, though restricted to the rotational degree of freedom, can still have entanglement introduced due to the long iteration run time. Adaptive learning rates and strategic restarts, triggered when entanglement entropy reaches a threshold (a very useful technique when trying to prevent over-entanglement in EBH models), can help the optimizer respond to low-gradient areas by adjusting step size as needed, preventing stagnation in flat regions.[38]

Furthermore, adjusting circuit structure—such as using shallow circuits or controlling expressibility via tdesigns—helps prevent barren plateaus by avoiding overparameterization and reducing entanglement. Dynamically adjusting circuit depth based on feedback maintains train-ability while mitigating gradient vanishing.[39]

Regularization techniques from classical ML, like penalizing large parameters, can help prevent overfitting to flat regions and keep the optimization landscape dynamic. Classical shadows and noise-aware methods adapt measurements to reduce noise impacts, addressing barren plateaus on quantum hardware.[36]

Finally, noise-resilient ansatz designs that restrict entanglement across qubits can help maintain gradient values. Parameter correlation, where parameters are linked or constrained, lowers optimization dimensionality and manages noise, while error mitigation techniques like post-processing adjustments help reduce noise effects. Together, these methods can help stabilize gradients and optimize the training landscape for scalable VQE implementations.

B. Balancing tractability and applicability in quantum simulations

Simulating black holes represents a formidable task at the intersection of quantum mechanics, general relativity, and quantum gravity. The extreme conditions and singularities inherent to black holes create significant challenges for quantum simulations. Conventional quantum simulation frameworks, typically suited to less extreme systems, fall short when it comes to capturing the intense gravitational fields and event horizons unique to black holes.

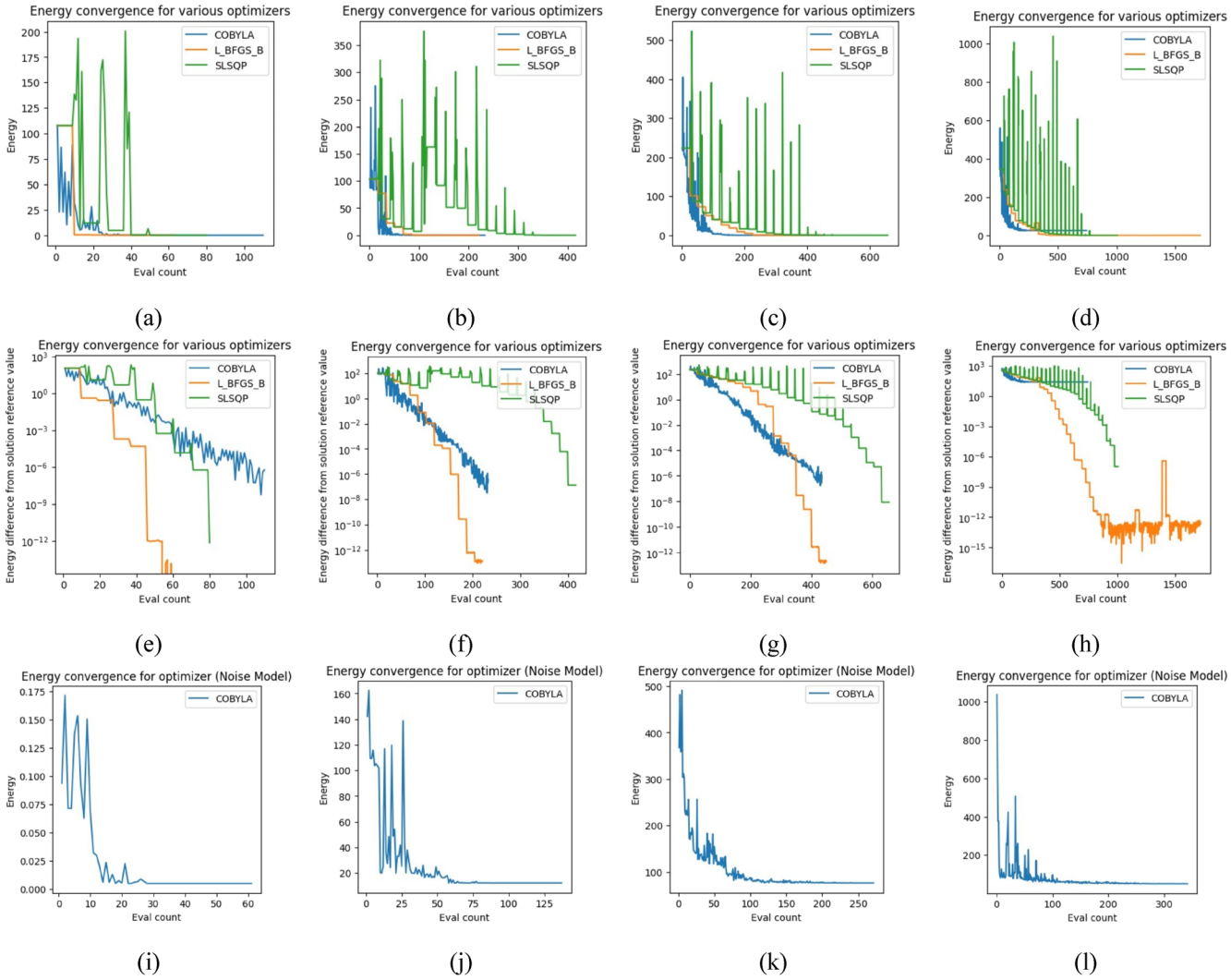

FIG. 3. Ansatz 1 results: The VQE results for different values of N for the custom ansatz have been provided. Figures (a)–(d) show the number of iterations each optimizer took to reach the minimum for the custom ansatz. Figures (e)–(h) show the difference between the optimizer results and actual energy. Figures (i)–(l) show the optimizer results for COBYLA after the application of the thermal noise model to the VQE estimator. Each column for figures corresponds to one value of N, with the value of N increasing from left to right [$N = 2$ for (a), (e), and (i); $N = 4$ for (b), (f), and (j); $N = 8$ for (c), (g), and (k); $N = 16$ for (d), (h), and (l)]. The eval counts seen on the x axis of the plots are the cost function evals, which are the number of iterations each optimizer took before reaching the convergence.

Current quantum resources permit only the implementation of simplified toys models. These models provide a tractable simulation framework within the constraints of present-day quantum processors, though they inherently limit applicability, particularly in scenarios involving late-stage evaporation where quantum gravity effects become essential.

A full quantum model of black holes demands a substantial number of qubits to represent the complex information dynamics of black hole formation and evaporation. Simulating a black hole requires not only modeling the black hole itself but also the entangled states of particles involved in its formation and decay.[40] Consequently, this demands a high-dimensional Hilbert space, significantly increasing quantum resource requirements as system complexity scales. While quantum computers could leverage quantum parallelism for simulating black holes, the scale of the required circuits is immense.

The thermodynamic properties of black holes and their implications for the information paradox form another core focus. Simulating black holes in a quantum framework necessitates a deep understanding of how information is encoded, resonating with foundational quantum mechanics and thermodynamics principles. Concepts like "black hole complementarity" and information scrambling through radiation are central to identifying the quantum resources needed for such simulations.

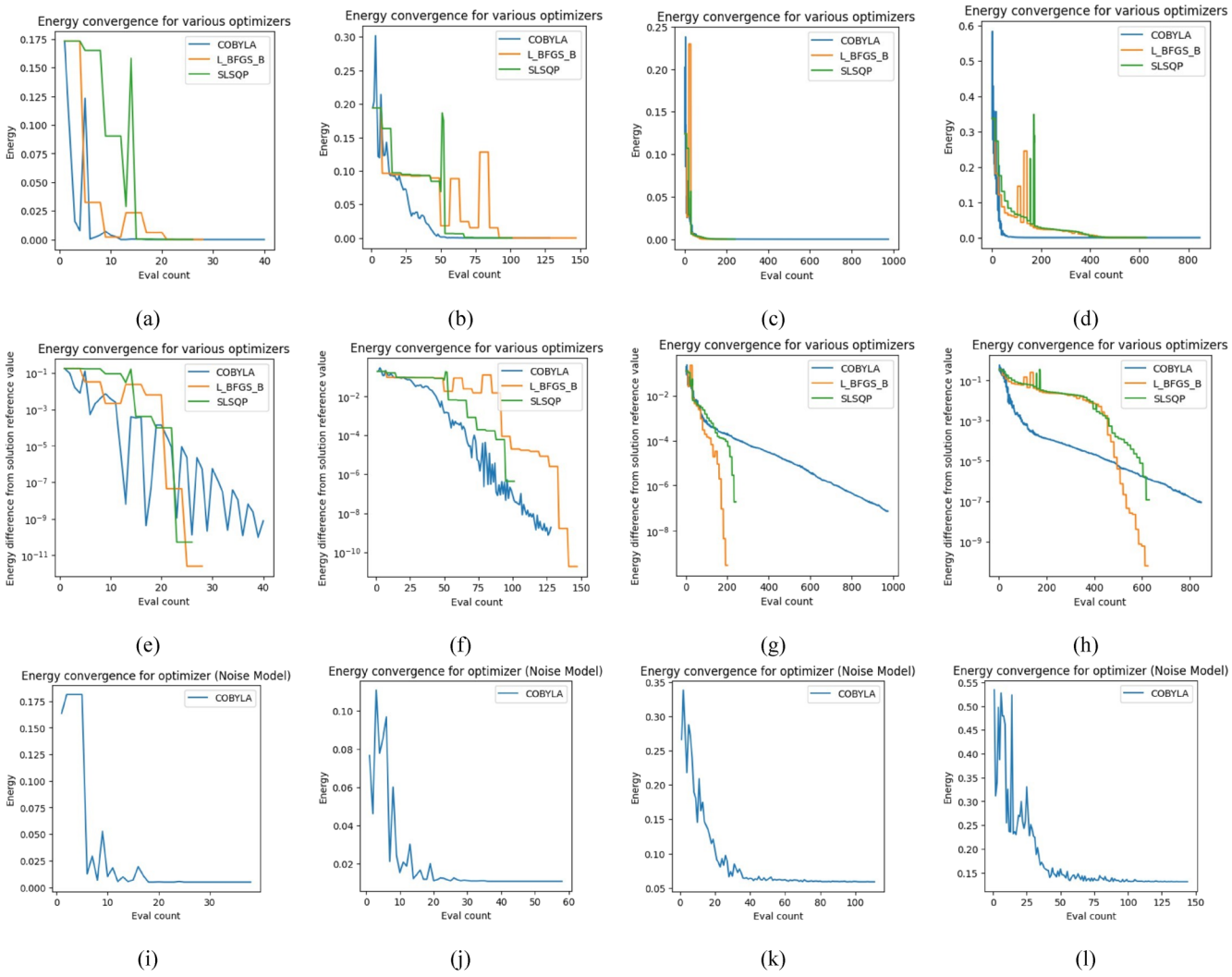

FIG. 4. Ansatz 2 results: The VQE results for different values of N for the TwoLocal ansatz have been provided. Figures (a)–(d) show the number of iterations each optimizer took to reach the minimum for the TwoLocal ansatz. Figures (e)–(h) show the difference between the optimizer results and actual energy. Figures (i)–(l) show the optimizer results for COBYLA after the application of the thermal noise model to the VQE estimator. Each column for figures corresponds to one value of N, with the value of N increasing from left to right [$N = 2$ for (a), (e), and (i); $N = 4$ for (b), (f), and (j); $N = 8$ for (c), (g), and (k); $N = 16$ for (d), (h), and (l)]. The eval counts seen on the x axis of the plots are the cost function evals, which are the number of iterations each optimizer took before reaching the convergence.

As a future direction that can be used as an approach to model a more realistic EBH simulation and gain relevant results, we wish to incorporate the effects of Hawking radiation by the method discussed in Sec. IV.

IV. DISCUSSION

There are shortcomings with the metric ansatz we have employed in this work. Since there is no relationship between time inside and outside of a black hole, this model is not an entirely accurate representation of EBH.

So far, black hole models have been developed using the Sachdev–Ye–Kitaev (SYK) model, which captures some chaotic aspects of black hole dynamics.[40] The SYK model requires qubits to interact in ways that replicate the non-locality of black holes, often demanding many qubits to represent even simple aspects of black hole physics. Recent work exploring the SYK model on quantum devices has shown that even a modest approximation requires hundreds of qubits and operations.

The AdS/CFT correspondence suggests that a lower dimensional quantum system (like a 2D conformal field theory) can replicate the physics of a 3D black hole.[40] Quantum simulators can exploit this relationship to reduce dimensionality and resource

requirements, making black hole simulations more feasible on current devices. However, even with dimensional reduction, achieving sufficient qubit fidelity and managing errors due to decoherence (especially in systems like trapped ions or superconducting qubits) remains challenging.

Additionally, thermal noise can introduce relaxation and dephasing, both major error sources in VQE. Relaxation drives qubits toward the ground state, disrupting coherence and state preparation, while dephasing reduces coherence by pushing qubits toward classical states, hindering superpositions essential for accurate computations.

As circuit depth and execution time increase, susceptibility to thermal noise rises. VQE's iterative nature compounds this effect, degrading result fidelity and limiting useable circuit depth. Lowered fidelity from thermal noise necessitates more samples (shots) for reliable results, escalating time and resources, particularly in larger systems. To improve scalability, larger quantum volumes and advanced EBH models could mitigate these noise impacts.

As mentioned before, we only considered the Hamiltonian due to the spacetime. However, to calculate the total Hamiltonian, we have to consider the Hawking radiation. To do so, we can discretize the spacetime (as performed in this article) and couple it with the methods in lattice QCD. Such a method,[41–46] combined with quantum computational methods, can help us calculate the Hamiltonian due to the Hawking radiation. That will not only complement our analysis but also enable us to work with the Vaidya metric as our choice of spacetime metric for EBH.

The lattice QCD method encodes QCD's gauge theories onto digital quantum computers using a simpler, finite dimensional Hamiltonian.[42] The gauge degrees are encoded into qubits using noncompact variables. Followed by developing a truncated Hamiltonian in the coordinate basis to facilitate quantum computation while utilizing a qubit-based representation for gauge variables. Implementing gauge fixing techniques can help reduce redundant degrees of freedom and simplify the Hamiltonian used in computations.[41] More details about EBH models can be studied in the cited Refs. 28–32.

As was mentioned earlier in Subsection II C, the ansatz used for the VQE protocol should be flexible enough so that it can reach the actual ground state wave function. It appears that the L-BFGS-B optimizer, which locates the input function minima where the variables are bounded, is well suited to the custom ansatz presented in this article. However, the same ansatz results in the barren plateau for $N = 16$ and the COBYLA optimizer. It also did not perform well for the noise model case. While the TwoLocal ansatz mostly outperformed for all the cases except the L-BFGS-B optimizer in terms of closer upper bound energy value.

VQE has drawn much interest in recent years because of its potential to solve challenging quantum mechanical issues, particularly in the fields of quantum chemistry and materials science. In this article, we covered the main concepts involved in the VQE algorithm.

- Variational Ansatz: VQE uses a variational ansatz, which is a parameterized quantum circuit intended to simulate the target quantum system's ground state. To reduce the energy expectation value of the system, the parameters in this circuit are iteratively optimized.
- Objective Function: The goal of VQE is to reduce the system's Hamiltonian expectation value, which represents the quantum system's overall energy. This objective function gauges how closely the ansatz resembles the actual ground state and is dependent on the variational parameters.
- Classical Optimization: In VQE, quantum and classical computations are combined. The variational parameters are updated iteratively to minimize the objective function using traditional optimization techniques.
- Quantum Measurement: For each cycle of VQE, the quantum circuit is measured in order to determine the Hamiltonian's expectation value. The classical optimizer can modify the variational parameters using the information from these measurements.

VQE simulates quantum systems more effectively than traditional computers by taking advantage of the parallelism that exists in quantum computing. VQE scales more favorably with the number of qubits, whereas classical algorithms for quantum simulation frequently suffer from the exponential growth in computer resources required as the system size increases.

The adaptability of VQE is another one of its main advantages. VQE is a quantum algorithm that does not necessitate an in-depth understanding of the features of the quantum system. Instead, it adapts to different systems by using a parameterized ansatz that may be modified to fit the unique needs of the current issue. Because VQE is hardware-independent, it can be used with various quantum computing architectures. This is essential in the current quantum computing environment, where a variety of quantum devices with diverse qubit designs and error rates are available. The superconducting qubit-based machine, the trapped-ion quantum computer, or any other technology can be used by researchers and practitioners to implement VQE.

The hybrid nature of VQE brings together the advantages of both classical and quantum computing. Classical computers handle the optimization work, whereas quantum computers carry out the quantum measurements and operations required for the procedure. VQE is more useful for current quantum devices thanks to this hybrid method, which makes use of both the classical and quantum systems' processing power. Due to issues including noise, gate errors, and decoherence, quantum computers are prone to errors. Through the use of techniques like error correction codes or error-resistant variational forms, VQE may be able to reduce some of these faults. Because of this, VQE is a strong contender for resolving practical issues even before fault-tolerant, error-corrected quantum computers are generally accessible.

The cost of performing quantum calculations is decreased by VQE's capacity to perform quantum simulation using a comparatively small number of qubits compared to other techniques. As a result, it is a viable option for simulating complicated quantum systems without the need for obscenely expensive quantum hardware. By its very nature, parallelism is used in quantum computing to speed up some calculations compared to their classical counterparts. This parallelism is exploited by VQE to explore many trial states concurrently, which can greatly accelerate the optimization process. VQE's potential for speedup increases as quantum hardware advances.

Quantum chemistry, condensed matter physics, and materials science can all benefit from VQE's capacity to tackle challenging quantum challenges. This interdisciplinary potential encourages interaction between researchers from other disciplines, resulting in novel discoveries and solutions. The precision and effectiveness of VQE implementations may be impacted by certain hardware limitations (connectivity issues, gate errors, and qubit count restrictions). The trustworthiness of VQE results must be ensured by the application of efficient error mitigation techniques, especially for big and complicated systems.

It is essential to select the right classical optimization algorithm for VQE. The efficiency and convergence behavior of various optimizers may differ, which could have an impact on the algorithm's overall performance. The success of VQE is greatly influenced by the variational ansatz's design. It takes domain-specific knowledge and expertise to select an ansatz that accurately represents the characteristics of the target quantum system. Quantum volume, which includes qubit count, gate integrity, and coherence duration, is a key element in figuring out how effectively a quantum device can carry out VQE. Increasing quantum volume will improve VQE's performance as quantum hardware develops. Although VQE scales better than classical techniques, it still has difficulties when used with large, highly connected quantum systems. A growing body of research is being performed on approaches for managing system scalability.

V. CONCLUSION

In conclusion, our exploration of the performance of the variational quantum eigensolver (VQE) algorithm using the Evaporating Black Hole (EBH) model has shed light on the potential and challenges of applying quantum computational techniques to the study of complex cosmological systems. Although the ingoing Vaidya metric turns out to be a more accurate ansatz for the EBH than the metric that was previously studied, the limitations of the metric ansatz used in this work highlight how difficult it is to fully describe the dynamics of an evaporating black hole within the framework of quantum mechanics.

VQE is a crucial asset in the present quantum computing landscape because of its versatility, hardware independence, and capacity to address real-world problems, even in the face of quantum hardware restrictions. However, our study reveals that the choice of the variational ansatz, the classical optimization algorithm, and considerations of quantum volume are crucial factors influencing the performance and reliability of VQE. The custom ansatz presented in this article, while effective with certain optimizers, exhibits limitations in scalability, highlighting the ongoing challenges in managing large, highly connected quantum systems.

VQE has the potential to solve challenging quantum puzzles and speed up scientific discovery as quantum technology develops and improves. The hybrid nature of VQE, which combines the benefits of both quantum and classical computing, also places it in a position to serve as a link between existing quantum technologies and the realization of the quantum advantage for real-world applications. A growing body of research is being performed on approaches for managing system scalability.

While concerns like hardware constraints and error mitigation continue to be a problem, continuous research efforts are devoted to solving these problems and further increasing the capabilities of VQE. As a result, VQE continues to be a crucial algorithm in the field of quantum computing, opening the door to new understandings of quantum systems and the creation of new materials and chemical compounds with revolutionary features.

In conclusion, VQE opens new avenues for exploring the frontiers of quantum mechanics, offering a glimpse into the future of computational methodologies that may redefine our understanding of the fundamental principles governing the universe.

ACKNOWLEDGMENTS

The support of IBM's quantum experience is acknowledged by the authors. The views expressed by the authors are their own, and they do not necessarily reflect the official position or guidelines of IBM or the IBMQ experience team. This work at Hampton University was supported by NASA Grant Nos. NNX15AQ03A and ARO W911NF-15-1-0535.

AUTHOR DECLARATIONS

Conflict of Interest

The authors have no conflicts to disclose.

Author Contributions

Ritu Dhaulakhandi: Conceptualization (equal); Data curation (equal); Formal analysis (equal); Investigation (equal); Methodology (equal); Validation (equal); Visualization (equal); Writing – original draft (equal). **Raikhik Das**: Conceptualization (equal); Data curation (equal); Investigation (equal); Methodology (equal); Validation (equal); Visualization (equal); Writing – review & editing (equal). **Bikash K. Behera**: Conceptualization (equal); Data curation (equal); Methodology (equal); Project administration (equal); Supervision (equal); Validation (equal); Visualization (equal); Writing – review & editing (equal). **Felix J. Seo**: Conceptualization (equal); Methodology (equal); Project administration (equal); Supervision (equal); Validation (equal); Visualization (equal); Writing – review & editing (equal).

DATA AVAILABILITY

All pertinent data that support the study's conclusions are provided in this article. Additional information can be requested from the authors if required.

REFERENCES

[1] P. Benioff, "Quantum mechanical models of Turing machines that dissipate no energy," Phys. Rev. Lett. **48**, 1581 (1982).
[2] Y. I. Manin, *Computable and Uncomputable* (Sovetskoe Radio, 1980), p. 128.
[3] R. P. Feynman, "Simulating physics with computers," Int. J. Theor. Phys. **21**, 467 (1982).
[4] D. Deutsch, "Quantum theory, the Church–Turing principle and the universal quantum computer," Proc. R. Soc. Lond. A **400**, 97–117 (1985).
[5] P. W. Shor, "Polynomial-time algorithms for prime factorization and discrete logarithms on a quantum computer," SIAM J. Comput. **26**, 1484 (1997).
[6] D. J. Griffiths, *Introduction to Quantum Mechanics* (Pearson Prentice Hall, 2004).

[7]A. Y. Kitaev, "Quantum computations: Algorithms and error correction," Russ. Math. Surv. **52**, 1191 (1997).
[8]B. K. Behera, S. Seth, A. Das, and P. K. Panigrahi, "Demonstration of entanglement purification and swapping protocol to design quantum repeater in IBM quantum computer," Quantum Inf. Process. **18**, 108 (2019).
[9]S. K. Rajiuddin, A. Baishya, B. K. Behera, and P. K. Panigrahi, "Experimental realization of quantum teleportation of an arbitrary two-qubit state using a four-qubit cluster state," Quantum Inf. Process. **19**, 87 (2020).
[10]A. Pal, S. Chandra, V. Mongia, B. K. Behera, and P. K. Panigrahi, "Solving Sudoku game using a hybrid classical-quantum algorithm," Europhys. Lett. **128**, 40007 (2020).
[11]R. G. Ingalls, "Introduction to simulation," in 2008 Winter Simulation Conference, 2008.
[12]I. M. Georgescu, S. Ashhab, and F. Nori, "Quantum simulation," Rev. Mod. Phys. **86**, 153 (2014).
[13]R. Laflamme and E. P. S. Shellard, "Quantum cosmology and recollapse," Phys. Rev. D **35**, 2315 (1987).
[14]P. Amsterdamski, "Wave function of an anisotropic universe," Phys. Rev. D **31**, 3073 (1985).
[15]P. Pedram, "On the conformally coupled scalar field quantum cosmology," Phys. Lett. B **671**, 1–6 (2009).
[16]S. W. Hawking and J. C. Luttrel, "Higher derivatives in quantum cosmology," Nuclear Phys. B **247**, 250–260 (1984).
[17]S. Capozziello and R. D. Ritis, "Minisuperspace and Wheeler–Dewitt equation for string dilaton cosmology," Int. J. Mod. Phys. D **2**, 373–379 (1993).
[18]C. D. Kocher and M. McGuigan, "Simulating 0 + 1 dimensional quantum gravity on quantum computers: Minisuperspace quantum cosmology and the world line approach in quantum field theory," in *2018 New York Scientific Data Summit (NYSDS)* (IEEE, 2018).
[19]J. B. Hartle and S. W. Hawking, "Wave function of the universe," Phys. Rev. D **28**, 2960 (1983).
[20]A. Ganguly, R. Dhaulakhandi, B. K. Behera, and P. K. Panigrahi, "Demonstration of minisuperspace quantum cosmology using quantum computational algorithms on IBM quantum computer," Quantum Inf. Process. **20**, 242 (2021).
[21]H. Y. Ku, N. Lambert, F. R. Jhan, C. Emary, Y. N. Chen, and F. Nori, "Experimental test of non-macrorealistic cat-states in the cloud," npj Quantum Inf. **6**, 98 (2020).
[22]A. Peruzzo, J. McClean, P. Shadbolt, M.-H. Yung, X.-Q. Zhou, P. J. Love, A. Aspuru-Guzik, and J. L. Obrien, "A variational eigenvalue solver on a photonic quantum processor," Nat. Commun. **5**, 4213 (2014).
[23]See http://www.research.ibm.com/ibm-q/ for IBM Quantum Experience.
[24]S. Hawking, "Black hole explosions?," Nature **248**, 30–31 (1974).
[25]See https://github.com/Qiskit/qiskit-aqua for Qiskit Aqua Library.
[26]A. Aste and D. Trautmann, "Radial fall of a test particle onto an evaporating black hole," Can. J. Phys. **83**, 1001–1006 (2005).
[27]R. Dey, S. Liberati, Z. Mirzaiyan, and D. Pranzetti, "Black hole quantum atmosphere for freely falling observers," Phys. Lett. B **797**, 134828 (2019).
[28]K. Kassner, "Radially falling test particle approaching an evaporating black hole," Can. J. Phys. **97**, 267–276 (2019).
[29]E. Balbinot and E. Bergamini, "A radiating metric for evaporating black holes," Nuovo Cimento B **68**, 104–110 (1982).
[30]S. Abdolrahimi, D. N. Page, and C. Tzounis, "Ingoing Eddington–Finkelstein metric of an evaporating black hole," Phys. Rev. D **100**, 124038 (2019).
[31]M. Beciu, "Evaporating black hole in Vaidya metric," Phys. Lett. A **100**, 77–79 (1984).
[32]J. Piesnack and K. Kassner, "The Vaidya metric: Expected and unexpected traits of evaporating black holes," Am. J. Phys. **90**, 37–46 (2022).
[33]V. K. Jain, B. K. Behera, and P. K. Panigrahi, "Quantum simulation of discretized harmonic oscillator," Quantum Stud. Math. Found **8**, 375–390 (2021).
[34]R. D. Somma, "Quantum simulations of one dimensional quantum systems," Quantum Inf. Comput. **16**, 1125 (2016), https://dl.acm.org/doi/abs/10.5555/3179430.3179434.
[35]See https://en.wikipedia.org/wiki/Main_Page for Quantum Fourier Transform.
[36]M. Larocca, S. Thanasilp, S. Wang, K. Sharma, J. Biamonte, P. J. Coles, L. Cincio, J. R. McClean, Z. Holmes, and M. Cerezo, "A review of barren plateaus in variational quantum computing," arXiv:2405.00781v1 (2024).
[37]A. Kulshrestha and I. Safro, "BEINIT: Avoiding barren plateaus in variational quantum algorithms," arXiv:2204.13751v1 (2022).
[38]S. H. Sack, R. A. Medina, A. A. Michailidis, R. Kueng, and M. Serbyn, "Avoiding barren plateaus using classical shadows," PRX Quantum **3**, 020365 (2022).
[39]L. Slattery, B. Villalonga, and B. K. Clark, "Unitary block optimization for variational quantum algorithms," Phys. Rev. Res. **4**, 023072 (2022).
[40]J. Maldacena, "A simple quantum system that describes a black hole," arXiv:2303.11534v3 (2023).
[41]V. Ale, N. M. Bauer, R. G. Jha, F. Ringer, and G. Siopsis, "Quantum computation of SU(2) lattice gauge theory with continuous variables," arXiv:2410.14580 [hep-lat] (2024).
[42]G. Bergner, M. Hanada, E. Rinaldi, and A. Schafer, "Toward QCD on quantum computer: Orbifold lattice approach," J. High Energy Phys. **2024**, 234.
[43]I. D'Andrea, C. W. Bauer, D. M. Grabowska, and M. Freytsis, "New basis for Hamiltonian SU(2) simulations," Phys. Rev. D **109**, 074501 (2024); arXiv:2307.11829 [hep-ph].
[44]K. Lee, F. Turro, and X. Yao, "Quantum computing for energy correlators," arXiv:2409.13830 [hep-ph] (2024).
[45]M. Rhodes, M. Kreshchuk, and S. Pathak, "Exponential improvements in the simulation of lattice gauge theories using near-optimal techniques," arXiv:2405.10416 [quant-ph] (2024).
[46]F. Turro, A. Ciavarella, and X. Yao, "Classical and quantum computing of shear viscosity for (2 + 1)*D* SU(2) gauge theory," Phys. Rev. D **109**, 114511 (2024); arXiv:2402.04221 [hep-lat].